

# Exploring The Inhibition Potential of FDA Approved Beta-Lactams and Their Newly Designed Derivatives Against Mycobacterium Tuberculosis: Molecular Docking, Validation, Molecular Dynamics Simulations and Ad-MET Predictions

Khair Bux<sup>2\*</sup>, Hassan Ahmed<sup>1</sup>, Usman<sup>1</sup>, Fareha Khalid<sup>1</sup>, Cem B Yildiz<sup>4</sup> and Ralf Herwig<sup>3</sup>

<sup>1</sup>Shaheed Zulfiqar Ali Bhutto Institute of Science and Technology (SZABIST), Karachi, Pakistan

<sup>2</sup>Department of Chemistry, University of Karachi, Karachi-75270, Pakistan

<sup>3</sup>Laboratories PD Dr. R. Herwig, 80337 Munich, Germany and Heimerer-College, 10000 Pristina, Kosovo

<sup>4</sup>Department of Medicinal and Aromatic Plants, University of Aksaray, Aksaray, Turkey

## \*Corresponding author:

Khair Bux,  
Department of Chemistry, University of Karachi, Karachi-75270, Pakistan,  
Email: khair.bux@szabist.edu.pk

**Received Date:** 17 May 2023

**Accepted date:** 03 June 2023

**Published Date:** 08 June 2023

## 1. Abstract

Tuberculosis (TB), caused by the bacterium *Mycobacterium tuberculosis* is one of the most prevalent diseases with an approximate of 10 million people having suffered from it in the year 2020. Furthermore, Pakistan ranks 6th for having one of the largest numbers of drug resistant TB each year. In the drug resistant cases, beta-lactamase is an enzyme that inactivates the beta-lactam ring in the drugs causing them to be inactive against the bacterium. MDR- resistance Tuberculosis has become a major threat worldwide. Drug repurposing is a successful approach in discovering new choices of treatment for preventing diseases by using pre-existing drugs. In this study, four Food and Drug Administration (FDA) approved drugs were repurposed against beta lactamase of *Mycobacterium tuberculosis*. Molecular docking was performed between the active sites of the beta-lactamase and drugs. Quantum mechanics analysis revealed electronic structural activity. Derivatives of these drugs were prepared and further docking was performed. 2-dimensional and 3-dimensional interactions results were obtained using Discovery Studio.

From the results, Sulfonamide and its derivative were found to have the best potency in terms of binding energy. Molecular docking simulations of Sulphonamide and its derivative were performed to check conformational stability of the protein-ligand complexes. Hence, further efficient analogs can be designed from the Sulfonamide drug and its selected derivative.

## 2. Keywords:

Beta-lactamases; FDA-approved drugs; Drug repurposing; *Mycobacterium tuberculosis*; MTB; In-silico analysis; Quantum Mechanics; Multi-drug Resistance

## 3. Introduction

Antibiotic resistance is threatened by tuberculosis (TB) produced by *Mycobacterium tuberculosis*, extensively drug-resistant tuberculosis (XDR-TB) and multidrug-resistant tuberculosis (MDR-TB). According to the World health organization WHO, IT was estimated that around 10 million individuals globally were infected with tuberculosis (TB). By 2020, there will be 5.6 million males, 3.3 million women, and 1.1 million children. Pakistan has the world's sixth-largest population and the fifth-highest TB burden. Every year, an estimated 27,000 drug-resistant TB cases are diagnosed. Our country Pakistan is considered and ranked on number sixth among one of the high-burden nations in terms of drug-resistant tuberculosis. A record of 369,548 persons have been diagnosed with tuberculosis (WHO Report, 2018). *M. tuberculosis* has a well-established potential to acquire medication resistance when combined with protracted treatment regimens. [1] Furthermore, the production of lactamase is regarded as one of the most important drivers of the development of intrinsic resistance to these antibiotics. [2] The formation of -lactamases, which break the amide bond in the target lactam ring, is one of the most efficient mechanisms of resistance to lactam antibiotics that are used against the disease (as seen in table 1).

**Table 1:** Drugs available for TB and its side-effects

Drugs	Mode of Action	Side Effects	Resistance Status
Isoniazid	Inhibit mycolic acid synthesis, which interferes with cell wall synthesis	Nausea, Vomiting, Upset stomach, Liver damage	MDR- TB
Rifampin	Inhibit bacterial DNA-dependent RNA polymerase	Upset stomach, heartburn, nausea, menstrual changes, or headache	MDR
Ethambutol	Inhibits arabinosyl transferase	Itching or rash; Joint pain; Headache, dizziness.	MDR
Pyrazinamide	Inhibits the synthesis of fatty acids; this disrupts the cell membrane	Nausea, vomiting, loss of appetite, or mild muscle/joint pain.	MDR

Considering some of the past years, there is a significant increase in the number of beta lactam resistant and many other strains of harmful pathogenic bacteria. [3] Resistance to -lactams is primarily caused by plasmid-derived lactamase genes being horizontally transferred [4]. The most prevalent mechanism of bacterial resistance to lactam antibiotics is the easy hydrolysis of the amide group of the lactam ring by -lactamases [5]. The 2019 AR Threats Report included antibiotic-resistant *Acinetobacter baumannii*, *Pseudomonas aeruginosa*, *Mycobacterium TB*, *Staphylococcus aureus*, and *Enterobacter* ales. The report issued a warning about the dangers of diseases caused by these germs (CDC).

In this regard, recent investigations indicated that deletion of chromosomal class A (Ambler) -lactamase, produced from the *M. tuberculosis* BlaC gene, increases susceptibility to *M. tuberculosis* by 8-256-fold. [6] The growing body of evidence for -lactamases, as well as the availability of information on their protein and subsequently nucleotide sequences, indicated that there are several classes of -lactamases, rather than a single homogeneous set of these enzymes. Furthermore, when enzyme activity against diverse lactam substrates was observed, it became obvious that -lactamases had a diversity of biochemical properties. Lactamases are classified into four types on the basis of the sequence of these amino acids' homology and general catalytic capabilities of enzymes. Here, D, A, and C are dependent on zinc or metallo—lactamases (MBLs; class B). Despite the fact that all four classes of clinically relevant and environmental bacteria are widely distributed, only a few enzyme families within each class have achieved extraordinary success and spread widely among the most important bacterial pathogens.

Penicillin's activity was previously reported to be much greater in class A-lactamases than Cephalosporinase's activity. Class A Serine -lactamases inactivate -lactams by an acylation-deacylation mechanism triggered by a nucleophilic attack on the active series, with Glu166 acting as the activating base. However, numerous novel class A -lactamases have

been discovered that are very active against newly formed generations of carbapenems and cephalosporins. To distinguish them from non-ESBLs, they are usually classified as extended-spectrum -lactamases (ESBLs) [7]. Class D-lactamases can block Ceftazidime, Cephalosporins, Penicillins, Cefotaxime, and other antibiotics. The hydrolysis of Carbapenem drugs such as Imipenem by class D -lactamases is a significant impediment to treating clinically significant infections. A Zn ion is coupled to metal linker amino acids in the active site of the metallo—lactamase group. Polarised water molecules aid in the breakdown of the lactam ring. The extensive use of lactams, like other antibiotic families, has resulted in the formation and spread of resistance. Cell permeability can be reduced (by inhibiting porins required for lactam's entry), efflux systems can be overexpressed, and modifying or degradative enzymes can be created if the target is changed (through mutation or transcription of alternative PBPs). The activity of lactamases, which are enzymes produced by enzyme-mediated resistance to the lactams is caused by Gram-negative and Gram-positive bacteria that hydrolyze the lactam amide.

Finding a safe and effective anti-tuberculosis therapy to treat extensively drug-resistant (XDR-TB) and multidrug resistant (MDR-TB) strains looks to be a difficulty. *M. tuberculosis* strains that are truly resistant to control have evolved as a result of the abuse of first-line beta lactam medicines.

Even though the exterior cell wall of *M. TB* was assumed to be a nearly-lactams have recently been shown to easily break the *M. tuberculosis* cell wall and bind the penicillin-binding proteins [8]. The respective gene in the *Mycobacterium tuberculosis* genome that has any detectable similarity to any of the known lactamase genes is BlaC (Rv2068c). As studies mentioned, The Pavelka group found that removing the BlaC gene increased *Mycobacterium tuberculosis* sensitivity to lactam antibiotics by showing folding to 8 to 256-fold, demonstrating BlaC's important involvement in *M. tuberculosis* resistance. Partially pure *Mycobacterium*

tuberculosis BlaC was formerly classified as a class A-lactamase subtype 2b because of its relatively high degree of Penicillinase activity. To thoroughly define *Mycobacterium tuberculosis* BlaC and aid in the development of novel inhibitors, we identified the substrate and inhibitor composition for BlaC as well as the structure of BlaC to high resolution [9].

The most common classification is based on sequence - based similarities, with four primary lactamase classes discovered, namely, A, B, C, and D. Three of them, classes A, C, and D, are serine-lactamases because the reactive nucleophile is a functional serine residue, while enzymes of class B are zinc-dependent hydrolases. Serine—lactamases use covalent catalysis to hydrolyze -lactams in a multistep method that involves the creation of several enzyme adducts. Serine-lactamases use covalent catalysis to hydrolyze -lactams in a multistep method that involves the creation of several enzyme adducts (Figure 2A). [9]

Many lactam antibiotic-lactamase inhibitor combos are now licensed for clinical usage, and many more are in late stage clinical development. [10]. Most of them combine a lactamase inhibitor with a cephalosporin derivative for broad-spectrum efficacy and lower hydrolysis susceptibility as compared to penicillin analogues [11]. There are numerous classes of -lactamase; in the case of *M. tuberculosis*, the lactamase is BlaC, which belongs to Amber class A. BlaC, *Mycobacterium tuberculosis*' lactamase, has been identified as the primary resistance determinant to lactam antibiotics, and successful suppression restores susceptibility [12]. More recently, increased worry over drug-resistant tuberculosis has coincided with advancements in the field of lactamase drug discovery and development, encouraging researchers to investigate the topic of whether a combination of lactam and lactamase inhibitors might successfully treat *M. tuberculosis*. [12] B-lactam antibiotics impede the last steps of peptidoglycan formation by combining with penicillin binding proteins (PBPs) in the membrane of a cell of bacteria to form an enzyme complex of stable acyl enzymes.

Gram-negative bacteria, on the other hand, have exploited three primary mechanisms to development of resistance against b-lactam antibiotics: (1) structural alteration of Penicillin - binding protein targets, (2) production of b-lactamase, and (3) aggressive evacuation of b-lactam drugs through efflux pumps. Penicillin binding proteins (PBPs), which accelerate the processes involved in the development of the bacterial cell wall, are the targets of B-lactam antibiotics. Transpeptidases (high - molecular - weight [hmv] PBPs) and D-alanyl-D-alanine-carboxypeptidases (low - molecular - weight [lmv] PBPs) are the two types of PBPs (DD-carboxypeptidases). *S. pneumoniae* has six penicillin binding proteins in their structure those are: PBP1a, PBP1b, PBP2a, PBP2b, PBP2x, and PBP3. Changes to one or more of these six PBPs' penicillin-binding domains shows their result in b-lactam antibiotic resistance in *S. pneumoniae*. PBP1a, PBP2b, and PBP2x are the three most amazingly significant types of PBPs for antibiotic resistance in b-lactams. MRSA can develop resistance to b-lactam antibiotics because it contains PBP2a which has been initially altered to have a low level of affinity for them. *S. pneumoniae* and MRSA

are resistant to b-lactam antibiotics, even when treated with a limited number of cephalosporins and carbapenems, according to several studies.

## 4. Chapter 2

### 4.1. Drug Repurposing

#### 4.2. How and why new drugs are useful against new targets

To reduce the difficulties of treating tuberculosis, we urgently want innovative medications with mechanisms that can be treated as well as can help in shortening the treatment strategy for both drug-susceptible strains, and the drug-resistant strains which might be more easily tolerated and may improve its adherence to therapy. However, due to the time and expense associated with the various processes, designing more effective TB treatment regimens is highly complex and time-consuming. As a result, pharmaceutical firms and scientists are focused on discovering interactions between new medications and targets by repurposing existing pharmaceuticals that have previously been used to treat a range of conditions, a process known as drug repurposing.

Drug repositioning, also known as drug repurposing, is the process of discovering new therapeutic uses for drugs that are previously recognized and approved. This technique decreases the chance of failure, shortens the time necessary for new drug development, requires less expenditure, and may lead to the discovery of fresh targets for further pharmaceutical research. [13]

Drug repurposing offers a highly appealing technique in tuberculosis therapy to address the issue of therapeutic resistance as it occurs and to discover drug candidates that can decrease the duration of treatment (TB). This method will eventually prevent the establishment of resistance and ensure the regimen's survival. Medication repurposing is significantly transforming translational research by ensuring thorough safety and effectiveness while lowering the time necessary to cross regulatory obstacles.

Additionally, there is continuing research on the use of immunomodulators as an adjuvant therapy using the traditional DOTs (Directly Observed Treatment, Short-course) treatment with the only goal of reducing treatment duration as well as pulmonary toxicity. [14] These additional medicines are intended to prevent TB disease reactivation and reinfection. The vast majority of repurposed medications offer minimal safety concerns, making them ideal candidates for immunomodulators. Their usage as immune modulators in combination with the normal anti-TB treatment may help to clear the infection fast and efficiently.

In this section, we will go through the detailed analysis of each of these repurposed medications, their mode of action, and any possible immunomodulatory effects. Figure 1 depicts the many strategies for using medications to treat various ailments (Figure 1).

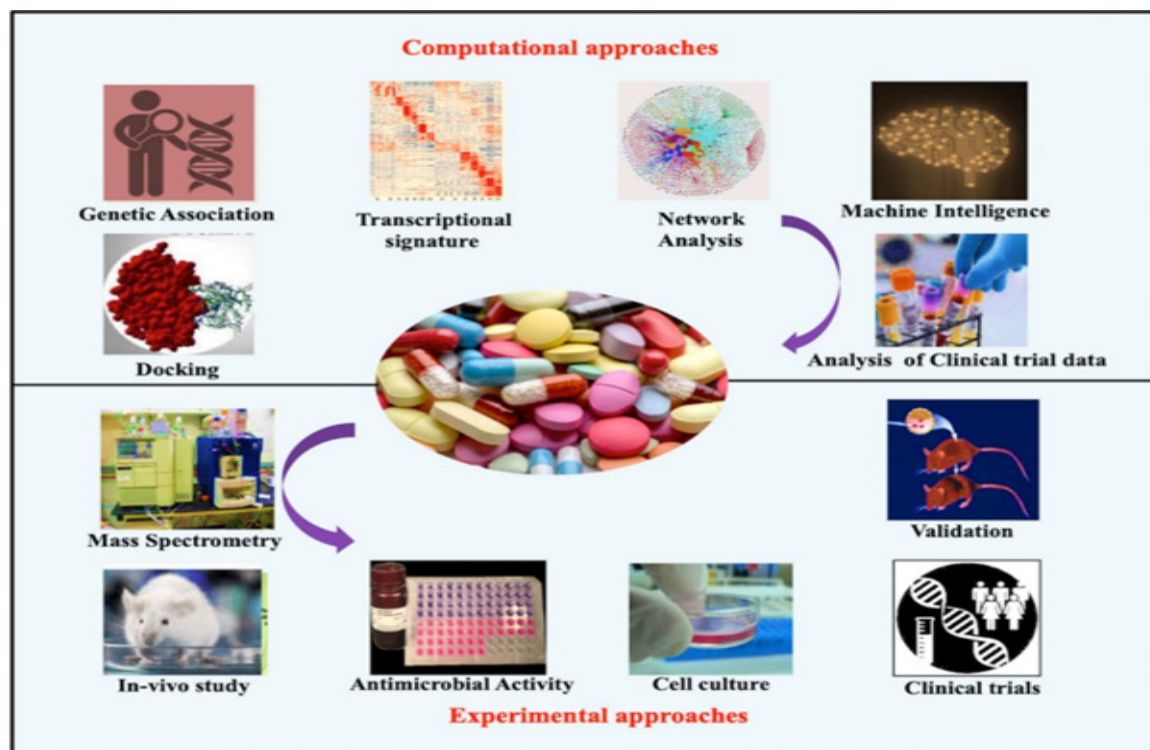


**Figure 1:** Different techniques to use medications for the treatment of diseases

### 4.3. Drugs and their derivatives used in the current study background and reason for repurposing against MTB

#### 4.3.1. Sulfonamide and derivative

Sulfonamides, also known as sulfa medicines, are strong antibacterial antibiotics and their spectrum of activity is extremely broad against so many gram-positive and gram-negative bacteria. Sulfonamides and derivatives of sulfonamides were collectively given as monotherapy from the 1930s until the 1950s but were eventually phased out due to their limited effectiveness compared to streptomycin and INH and its severe toxicity [14, 16]. These drugs can be studied further for usage in the treatment of TB by further study involving diverse groups of humans as subjects. More study on how they affect the immune system is needed because there isn't much evidence to support their role as immunomodulators.

Co-trimoxazole, popularly known as Sulfamethoxazole (sulfonamide)-trimethoprim (diaminopyrimidine), has been utilized in the treatment of drug-resistant TB. Co-trimoxazole has been shown to be extremely effective against drug-resistant MTBs both in vivo and in vitro (Palomino and Martin 2016). This information has prompted us to consider sulfonamides for their possible action against the unconfirmed beta lactamase of MTB.

#### 4.3.2. Cefixime and derivative

Cefixime, a third-generation cephalosporin that may be administered orally, displays antibacterial activity in vitro against the majority of the common lower respiratory infection *Moraxella catarrhalis*, *Hemophilus influenzae* and *Streptococcus pneumoniae* are all susceptible to the medicine, however *Staphylococcus aureus* is not. Because of its long

elimination half-life, Cefixime can be given once daily (3 hours as opposed to 0.5 hours and 1.5 hours for Cefaclor and Cephalexin, respectively). According to computational studies, Cefixime, Etoposide, and Nebrodenside can all be used as efficient COVID-19 inhibitors [17]. The medicines demonstrated significant binding interactions in active protein pockets. Docking and modelling yielded more encouraging findings for Etoposide. The docking scores and binding energies of three protein complexes with Etoposide medication were recorded at their lowest levels. Cefixime's binding energy was -6.4.

#### 4.3.3. Cefadroxil and derivative

Historically, generations of successful cephalosporins were intended to promote broad-spectrum action and combat drug resistance in a number of non-Mtb infections. [18] These structural modifications appear to have altered their anti-mycobacterial actions, most likely due to unrelated, distinct characteristics of the mycobacterial cell wall. Early investigations found a SAR for Mtb, phenyl moieties or Pyridyl in a cephalosporin C7 position at the side chain were associated with anti-tuberculosis efficacy [19]. Using the most recent commercially available cephalosporins, we arrived with such a qualitative SAR. According to a correlation of Cefadroxil and Cephapirin, a hydrogen bond acceptor at the 4 position of the right-side (RHS) aromatic ring was also revealed to be favorable for activity, either as a hetero atom within the aromatic ring or as a hetero atom outside the aromatic ring cycle or an extra cyclic group as like a hydroxyl (in the cephalexin and cephapirin series, respectively).

A drug like this would prevent the resistant genes of enriched beta-lactam in the gut flora. Mtb selectivity may reduce the gastrointestinal adverse effects of broad-spectrum beta-lactam antibiotics. This particular method,

although useful and promising, would operate independently of our high-speed repurposing aim, which calls for the rapid introduction of novel TB medications.

#### 4.3.4. Cephadrine and derivative

It's worth noting that the molecule has the same active cyclohexadiene as Cephadrine's RHS. These findings suggested widespread, generation-

**Table 2:** Details and characteristics of the selected drugs

Drug	Common name	Class	Protein target	Therapeutic indications	Side effects
Cefixime	Suprax	Cephalosporin	PBPs	Gastroenteritis	Diarrhea. Stomach pain.
Cefadroxil	Duricef	Cephalosporin	PBPs	Pneumonia, skin infections, tonsils	Nausea, Vomiting, Diarrhea, Stiff or tight muscles, Joint pain,
Cefradine	Velsef	Cephalosporin	PBPs	Sinusitis, bronchitis	Tightness in your chest; Unusual bleeding; Seizure jaundice
Sulfisoxazole	Gantrisin	Sulphonamide	Dihydropteroate synthase	UTIs, bronchitis, eye infections	Lethargy. Anorexia. Nausea.

## 5. Methodology

### 5.1. Molecular Modeling

Molecular modelling (MM) is an in-silico method that uses computers to simulate the drawing, manipulation, and other features of compounds that rely on their three-dimensional (3D) structures. Exploration of molecular systems, from tiny chemical systems to enormous biological molecules, is done with these techniques. MM integrates a number of disciplines, including material science, nanostructures, drug design, and computational biology (Pimentel et al., 2013). Even though the simplest computations can be done by hand, but for any substantially complex system that requires molecular modelling, computers are inevitably needed. Additionally, it aids in understanding the fundamental ideas behind physical and chemical interactions, which are difficult to compute using experimental techniques. It also helps with the development of original theories, model representations, practices, as well as products. All molecular modeling techniques share the representation of the molecular systems at the atomistic level [3]. The most popular simulation methods in MM are Monte Carlo, geometry optimization, and molecular dynamics. Because Monte Carlo simulation utilizes random variables as model parameters rather than fixed variables like other simulation approaches,

independent chemical pathways for particular Mtb activity.

The majority of the cephalosporins examined showed synergy with rifampicin; the highest synergies were shown with the first-generation cephalosporins Cephadrine, Cephalexin, and Cefadroxil (with the exception of cefditoren, pivoxil, ceftibuten, and cefuroxime) (Table 2).

it varies from standard MM simulation techniques. RiskAMP is the name of the Monte Carlo simulation engine for Microsoft Excel. MM is being used in a variety of industrial applications. Estimation of the hydrocarbon content in crude oil's screening is one such example. American Petroleum Institute gravity, peptide nucleic acid, and distillation curve content are only a few examples of the raw data from crude oil that MM uses to build a hydrocarbon molecules model that matches quantifiable physiochemical properties of crude oil [5]. The chemical compositions of model hydrocarbon molecules, which are produced from profile data of the crude oil, are also used to interpolate, extrapolate, and predict crude oil tests and attributes on the basis of molecular thermodynamic models [2].

Inorganic, biological, and polymeric systems' structure, dynamics, surface characteristics, and thermodynamics are increasingly often studied using molecular modelling techniques. There are currently many readily accessible molecular force field models in databases [4]. Some of the biological processes that have been investigated using molecular modeling include protein folding, enzyme catalysis, protein stability, conformational changes related to biomolecular function, and molecular recognition of proteins, DNA, and membrane complexes [6]. There are three ways to predict the target protein structure on the basis of how similar the query sequence is to the PDB database: homology modelling, threading, and

ab initio modelling, which are used when the query sequence has less than 30% similarity to the PDB database. For homology modelling, there are several online and standalone bioinformatics programmes accessible, such as MODELLER, SWISS-MODEL, MODBASE, ProModel, etc., whereas for threading and ab initio, there are good platforms in I-TASSER, FUGUE, mGENThreader, Phyre, etc., and ROSETTA [7].

## 5.2. Quantum Mechanical Methods For Ligand Protein Modeling

For drug discovery and design, precise models for estimating the binding free energy between tiny molecules and proteins are required. Quantum mechanical techniques are becoming more and more common in the domain of computer-aided drug designing (CADD), which isn't merely a result of ever improving processing power but also because first-principles QM is supposed to have the highest accuracy [12]. Due to the first-principle characters of them, the laborious quick semi-empirical approaches as well as the ab initio methods are both free from the drawbacks of the force field's (FFs) fixed-charge approximation and the ball and spring description [9]. Use of QM techniques throughout the entire Computer-Aided Drug Design (CADD) process has been predicted to become a reality. The interest in QM in CADD has, at the same time, sparked further methodological development of QM techniques, including QM approaches that are involved in scoring, docking, improving recognized potential leading compounds, along with figuring out the mechanism of reaction [10]. For instance, QM calculations were carried out to look into notable variations in the affinity for binding upon converting a CH<sub>2</sub> linker into a carbonyl [13].

Quantum mechanics provides the correct analytical account for the electrons' activity and, consequently, of their chemistry. Theoretically, any atom or molecule's property can be accurately predicted using quantum mechanics (QM). Only systems containing a single electron have the QM equations ever been solved precisely in practice. Numerous methods have been used to approximation the solution for multiple electron systems [11]. These estimates can be very useful, but the researcher must have some understanding to understand whether every single estimate is true and accuracy the results would likely to be having.

Schrodinger and Heisenberg created two comparable formulations of quantum mechanics. Since the Schrodinger form serves as the foundation for almost all computational chemistry techniques, we shall simply provide it here. Schrodinger's paradox is:

$$\hat{H}\Psi = E\Psi$$

Here, E is the energy, C represents wave function, and Hamiltonian operator is H. These sorts of equations are referred to as an Eigen equation in mathematics. Then, C is referred to as the eigenfunction and E as the eigenvalue. However, this is not necessarily the case. The operator and eigenfunction can both be matrices.

The electron and nuclear locations affect the wave function C. As the name

suggests, an electron is described as a wave in this context. The behavior of electrons is described probabilistically in this way. As a result, it is able to describe the likelihood that electrons will be found in particular places but is unable to pinpoint their precise location. Since the wave function square provides estimates, the wave functions are often referred to as a probability amplitude. The only rigorously valid interpretation of a wave function is this one. If the wave function is continuous, normalizable, antisymmetric, and single-valued with regard to the electron exchange, the Schrodinger equation can be easily solved physically.

The Hamiltonian operator  $\hat{H}$  is, in general,

$$\hat{H} = - \sum_i^{\text{particles}} \frac{\nabla_i^2}{2m_i} + \sum_{i<j}^{\text{particles}} \sum \frac{q_i q_j}{r_{ij}} \quad (2.5)$$

$$\nabla_i^2 = \frac{\partial^2}{\partial x_i^2} + \frac{\partial^2}{\partial y_i^2} + \frac{\partial^2}{\partial z_i^2} \quad (2.6)$$

Here,  $\nabla^2$  or the Laplacian operator is operating upon particle *i*. Electrons and nuclei are both types of particles. The mass and charge of particle *i*

are denoted by symbols  $m_i$  and  $q_i$ , while the separation between them is

denoted by  $r_{ij}$ . Within a wave formulation, the particle's kinetic energy is provided by the first term. The energy resulting from a particle's Coulombic attraction or repulsion is the second term. The time-independent, non-relativistic Schrodinger equation is used in this formulation. Additional terms in the Hamiltonian may appear when relativity, interactions with electromagnetic radiation, or fields are considered.

$$\hat{H} = - \sum_i^{\text{electrons}} \frac{\nabla_i^2}{2} - \sum_i^{\text{nuclei}} \sum_j^{\text{electrons}} \frac{Z_i}{r_{ij}} + \sum_{i<j}^{\text{electrons}} \sum \frac{1}{r_{ij}} \quad (2.7)$$

The kinetic energy of the electrons is the first term in this equation. Another concept is the affinity of electrons to the nuclei. Electron repulsion makes up the third phrase. At the conclusion of the calculation, the energy is increased by the nuclei's attraction to one another. By viewing the entirety of this construct as the lead energy surface that nuclei travel on, the motion of nuclei can be explained.

Any molecule-specific property can be determined once a wave function has been established. This is accomplished by utilizing the operator's expectation value for that property, marked by the angled brackets  $\langle \rangle$ .

$$\langle E \rangle = \int \Psi^* \hat{H} \Psi \quad (2.8)$$

This is the energy that the Schrodinger equation predicts for an exact solution. This provides an approximation of the energy for an approximate wave function, which serves as the foundation for many of the techniques

detailed in later chapters. Because it always exceeds or is equal to the exact energy, this is known as variational energy. By substituting alternative operators, it is possible to obtain different observable qualities, such as the dipole moment or electron density. The frequently used computational chemistry methods only use the Hamiltonian to obtain the wave function. The Hellmann-Feynman theorem can also be used to determine molecular characteristics. According to this theorem, the energy derivative in regards with a certain property/characteristics P that is presented by:

$$\frac{dE}{dP} = \left\langle \frac{\partial \hat{H}}{\partial P} \right\rangle \quad (2.9)$$

For calculating electrostatic characteristics, this relationship is frequently utilized. The Hellmann-Feynman theorem is not always followed. The Hellmann-Feynman theorem is only adhered to by variational approaches [8].

### 5.3. Molecular Docking

With the use of high-throughput screening procedures, which use in vitro tests to gauge the activity of a large number of compounds against the target, medications are typically discovered by accident through a process of trial and error. This procedure takes a long time and costs a lot of money. Nevertheless, simulated molecular docking can be a helpful tool in the drug development process if the target's three-dimensional structure is known. By virtually screening compound databases, this in silico method makes it easier to identify interesting medication candidates.

The drug candidates discovered by the virtual screening procedure can then be further investigated using laboratory experiments (synthesis), toxicological testing, clinical trials, and further protocols.

Molecular docking is an essential tool in the field of structural molecular biology as well as in the computer-aided drug designing. Predicting the dominant binding mode(s) of a ligand with a protein having a known three-dimensional (3D) structure is the goal of this ligand—protein docking. Effective docking techniques locate high-dimensional spaces and make use of a scoring algorithm that would fairly score the potential dockings. With the help of that docking, massive libraries of compounds can then be virtually screened, the results can be ranked, and structural theories about how the ligands inhibit the target can be proposed. This information is crucial for lead optimization. Analyzing the outcomes of stochastic search methods can occasionally be ambiguous, and setting up the input structures for the docking is just as important as the docking itself [1].

Docking techniques typically employ an energy-based scoring system to identify the ligand conformation that is bound to the target that is energetically most beneficial. In general, it is believed that better protein-ligand binds result from lower energy scores than from higher energy values. It is possible to think about molecular docking as an optimization problem because its objective is to find the ligand-binding mode with the lowest energy. Figure (2) in [12] depicts the approach taken in the current study (Figure 2).

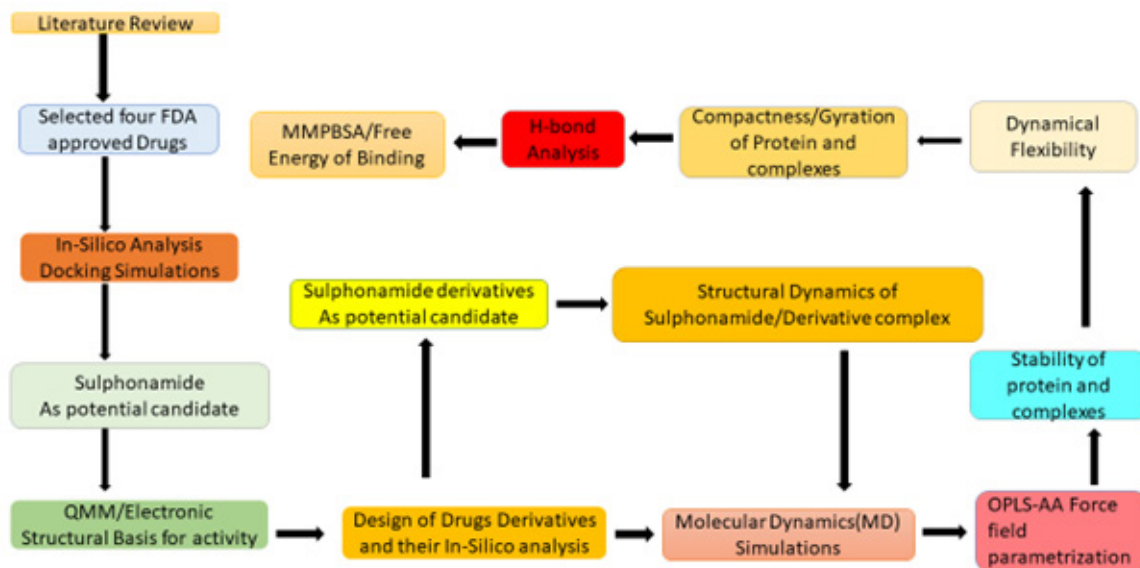


Figure 2: Work flow of the study

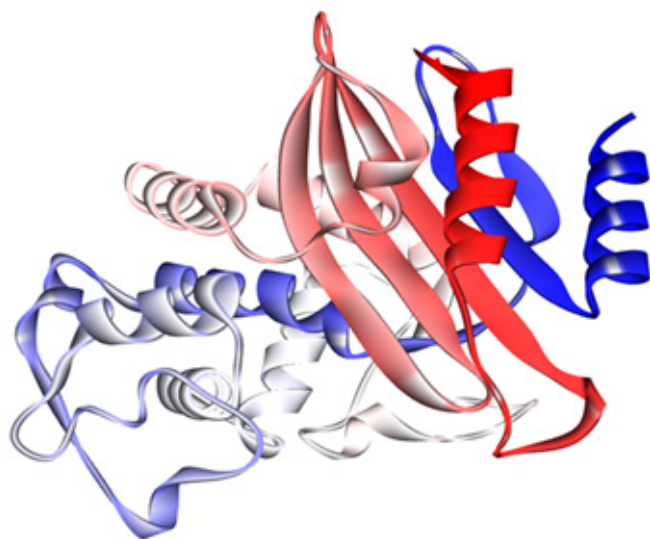
### 5.3.1. Ligand Preparation

A literature review and databases were used to gather the Drugs' structural information, which was then acquired from the PubChem database (<https://pubchem.ncbi.nlm.nih.gov/>) (Bekhit & Bekhit, 2014). The protein data bank format of the canonical smiles for the ligands was obtained and used for docking. The same process was utilized to recover the drug derivatives' structures, which were then employed for docking. The structures were then utilized as standard to compare with each other.

### 5.3.2. Protein Preparation

The 3D construction of beta lactamases responsible for developing antimicrobial resistance development was obtained from the Protein Data Bank database (PDB) (<https://www.rcsb.org/>) PDB ID 3N7W. The C-terminal denoted in red and N-terminal in blue color (Figure 3)[3].

**Figure 3:** Three-dimensional structure of the main beta-lactamases protein (PDB Id: 3N7W)



### 5.3.3. Initializing and putting PDBQT files together

The starting directory was set to the appropriate folder prior to docking. The finished protein molecule was loaded into the workspace of AutoDock 4.2.6. After the polar hydrogen atoms were added, the protein's Kollman and Gasteiger charges were calculated. The target was the protein after it had been saved in PDBQT format. The ligand was brought into the workstation, the root of the torsion tree was selected, the number of rotatable bonds was determined, and the data was saved in PDBQT format. In order to continue the simulation procedure, the ligand and protein were loaded into the workspace in PDBQT format.

### 5.3.4. Grid Specification

The predicted active site was similar to the 2-dimensional (2D) LigPlot of the co-crystallized protein that was in complex with the Amoxicillin. The process was done to assure the ligand being perfectly attached to the active site of the protein active site. Setting up the grid parameters is the one of the significant steps in molecular docking as it explores the ligand

with the binding site of the protease. The spacing of Grid was set to 0.375 Å (default). Center grid box values were -11.432, -9.16, and 2.636. The points for grid numbers in accordance with the x, y, and z dimensions was set to be 60, 60 and 58. There were 431893 total grid points on each map. The full 3-dimensional active site of the receptor was covered by these characteristics. The grid parameter file (GPF) file format was used to save the output. The set grid size and locations closely matched those given by Odhar et al., 2020 and Yu et al., 2020.

### 5.3.5. Auto-grid and Auto-dock running

Executing the AutoGrid required the AutoGrid executable and GPF files, which were then transformed to the grid log file. After then, the grid was started. The genetic algorithm was reset to default after AutoGrid ran successfully, and is now as follows: i) the number of GA runs: 10; ii) population size: 150; iii) the number of energy evaluations: 2.5 million (2.0 Å clustered tolerance); and iv) the number of generations: 27000. The docking parameter file (DPF) file format was used to save the output of the Lamarckian genetic method. The AutoDock was run after the docking log file (DLG) was converted using the AutoDock executable and DPF files as input. The top 10 free binding energy energies for each run and the inhibitory constant were included in the final DLG file. The results were examined, ordered according to binding energies, saved in PDBQT format, and the complex with the lowest binding energy was saved in PDB format for additional investigation (Figure 4).

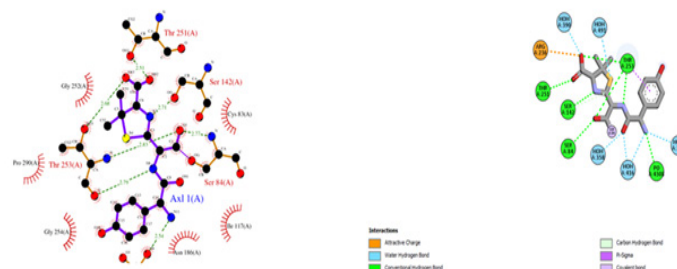


**Figure 4:** Two-dimensional (2D) interaction between protein and the ligands

### 5.3.6. Docking Validation

Utilizing two different techniques, the docking approach was validated. Using AutoDock 4.2.6, the complexed Amoxicillin was taken out and docked back into the active site (Alkhourairy et al., 2013). Manually, the co-crystallized complex was opened in a notepad, the inhibitor heteroatoms from the protein were removed, and the protein was then pasted into a new notepad and saved as an inhibitor in PDB file format. The method followed the same protocol, including the grid parameters. This was done in order to make sure that the inhibitor binds precisely to the active site cleft and must exhibit less deviation from the co-crystallized complex. The root mean square deviation (RMSD) was then computed by superimposing the re-docked complex with PyMOL 2.3 on top of the reference co-crystallized complex. This was done to assure the validation of docking and to validate the docking technique.





### 5.3.7. Molecular Dynamics Simulations

The Desmond package was used to do molecular dynamics simulations for the following complexes: free protein, protein complexes with sulfonamide, and protein complexes with its imidazole derivative. Following docking, the top two ligand-protein complexes had low binding energy. By putting the protein and the complexes in an explicit water box of size 10 with a single-point charge (SPC) water model TIP3P with periodic boundary condition, they were each independently solvated. The protein was modeled using the OPLS3e force field, and ligand, Na<sup>+</sup>, and Cl<sup>-</sup> ions were added to make the system's overall charge neutral (Harder et al., 2016; Sarma et al., 2020). Before a manufacturing run of 50 ns, the system was energy reduced for 2000 steps. Following reduction, the complex was further put through the NPT ensemble's manufacturing run. With the help of the Martina-Tobias-Klein method and the Nose-Hoover thermostatic algorithm, the system was gradually heated to maintain a temperature of 300 K and pressure. In order to simulate long-range electrostatic interactions with a grid spacing of 0.8 Å, the Particle Mesh Ewald (PME) approach was used. The intricate interactions between the ligand and protein were examined using the Simulation Interaction Diagram tool included in the Desmond package. Root mean square deviation (RMSD) and root mean square fluctuation (RMSF) measurements with respect to the reference were used to assess the results. Pant et al. reported the same process in 2020.

### 5.3.8. Free energy of binding: Molecular Mechanics Poisson-Boltzmann Surface Area (MMPBSA)

The ligand (drug) binding mode to the protein has generally been considered to be the drug binding mechanism [25]. In fact, Fisher's "lock-key" model, which sought to explain the intermolecular interactions between the ligand (drug) and the protein's amino acids in a specific area of the protein structure known as the binding site, offered the first elaboration of ligand's binding [24]. This static depiction of the ligand binding, however, suggests that the issue has been oversimplified. The ligand actually binds to the protein binding site in a dynamic process that begins with it binding from its fully solvated form and concludes with it unbinding and returning to the solvent.

Additionally, proteins have intrinsic dynamics and can adopt various conformations before to interacting with ligands (conformational selection) or particular conformations in response to ligand contact (induced fit). During this dynamic interaction, the ligand might assume binding poses that are energetically equivalent to the final binding mode, passing through high energy states that regulate the ligand binding and unbinding rate.

In the chemical reaction known as LPB, ligand L and protein P are referred to as reactants, and the complex LP that results from the ligand's binding to the protein is the product (Figure 1):

At equilibrium, the concentration ratio of reactants and product is constant in time and is equals to:

$$K_b = \frac{[LP]}{[L][P]} = \frac{1}{K_d} \quad (2)$$

Where  $K_d$  (in unit M) represents the dissociation (unbinding) constant  $K_b$  (in unit  $M^{-1}$ ) is a binding constant that is also considered as binding affinity, and the square brackets presents the equilibrium concentration of the molecular species (M unit).

The solute (i.e., protein and ligand), the solvent (i.e., water), and the buffer ions interact and exchange heat in the aforementioned reaction. The interactions between these molecules and the different types of energy they generate and exchange are controlled by the laws of thermodynamics, and they are frequently described in terms of Gibbs free energy G [23]. The latter is a thermodynamic potential that determines how much work may be reversed in a thermodynamic system at a given temperature and pressure. Therefore, LPB is only energetically favorable (i.e., spontaneous) when the difference in  $\Delta G^0$  system's Gibbs free energy between the bound and unbound states ( ) is negative after the system reaches equilibrium at a particular temperature and pressure.  $\Delta G^0$  the context of LPB, the absolute protein-ligand binding free energy, or  $\Delta G^0$ , is compared to  $K_b$  using the following formula:

$$\Delta G^0 = -k_b T \ln(C^0 K_b), \quad (3)$$

Where  $C^0$  is the standard concentration of 1 M for all the interacting molecules, which is useful for comparison with experiments, and  $k_b$  is the Boltzmann constant and T the temperature. The complex is clearly more thermodynamically stable with increasing binding constant  $K_b$  and decreasing standard free energy of binding, as shown by equation (3). It's also crucial to keep in mind that since  $\Delta G^0$  is a state function, the system's beginning and final states—irrespective of the path that associates them—determine it entirely. The differentiation in chemical potential among the complex ( $\mu_{LP}$ ) and the ligand and protein isolated ( $\mu_{LP}$  and  $\mu_P$ , respectively) can be used to calculate the  $\Delta G^0$ . A good expression of  $\Delta G^0$  using chemical potentials is given by statistical thermodynamics as indicated below:

$$\Delta G^0 = \mu_{LP} - \mu_L - \mu_P = -k_b T \ln \left( \frac{C^0 \int e^{-(U_{(rLP)} + S_{(rLP)}/k_b T)} dr_{(LP)}}{8\pi^2 \left( \int e^{-(U_{(rL)} + S_{(rL)}/k_b T)} dr_{(L)} \right) \left( \int e^{-(U_{(rP)} + S_{(rP)}/k_b T)} dr_{(P)} \right)} \right) \quad (4)$$

Here,  $U_{(rLP)}$ ,  $U_{(rL)}$ , and  $U_{(rP)}$  are the complex's, the ligand's, alongside protein's potential energies as functions of their respective coordinates

internally,  $r_{(LP)}$ ,  $r_{(L)}$ , and  $r_{(P)}$  (i.e., conformations), whereas  $S_{(rLP)}$ ,  $S_{(rL)}$ , and  $S_{(rP)}$  are their corresponding solvation energies. The rotational degrees of freedom of the solute (LP, L, and P) are taken into consideration

by the factor  $8\pi^2$ .

In this equation, all the conformations of the substances LP, L, and P should be considered; nevertheless, the integrals demonstrate greater contributions from more stable (low energy) conformations. It is also important to note that, in accordance with the law of mass action,

concentrations greater than  $C^0$  (1 M) result in least binding free energy values (more stable bound state). Therefore, when calculating the absolute

LPB free energy, methods should explicitly take  $C^0$  into account. On the other hand, if the relative binding free energy difference among the two

ligands is determined, it can be disregarded because in such case,  $C^0$  is cancelled.

A different way to state the Gibbs free energy  $\Delta G$  is as follows:

$$\Delta G = \Delta H - T\Delta S, \quad (5)$$

Here, S and H represent, respectively, the entropy and enthalpy differences between the bound and unbound states of the systems.

The LPB free energy is calculated using the various techniques covered in the following sections, using both Equations (4) and (5) (sometimes in different forms making explicit distinct energy contributions) [22].

## 6. Results & Discussions

This here-presented study is focused on Mycobacterium tuberculosis (MTB/TB) and finding a suitable drug candidate that can be used in its inhibition. For this purpose, we selected 4 FDA-approved drugs named Sulfonamide, Cefadroxil, Cefixime, and Cefradine. Furthermore, the derivatives of these drugs were also enrolled in this study and analyzed against the TB to determine its mode of interaction and inhibition against drugs.

To observe these interactions, the above-mentioned methods and techniques were used via various software and online tools, which in turn provided us with the recognition of the amino acids, bonding, and other important aspects that are necessary in the interaction.

Penicillin-binding proteins (PBP) are among the essential proteins present in the pathogen. PBPs play a key role in the synthesis of peptidoglycan, a crucial element of bacterial cell walls. There is a variety of modified PBPs present. Those modified PBPs causes the active site to change, which results in the  $\beta$ -lactam losing its affinity towards the target protein of the drug, hence, resistance occurs [64]. Among the latest therapeutic approaches, PonA1 is a potential target. It is a class A penicillin-binding protein, important for regulating the formation of the physiological cell wall as well as the cell shape during growth in MTB [65]. Hence, the PonA1 protein was used for docking against the FDA-approved drugs.

### 6.1. Molecular Docking

The docking of the resulting protein structure was performed using AutoDock4.2. AutoDock is basically a set of automated docking tools that is worn by the user. Using AutoDock, we were able to foresee and track how our protein structure interacted with the ligand in this investigation. The best confirmation received from that outcome was then used for additional examination, after which the structure with the best confirmation was used for re-docking. The confirmation with the highest binding score among the 250 confirmations was deemed to be the best confirmation.

In the case of the Cefixime drug, the binding energy was -4.52 in comparison to which Cefadroxil and its derivative had better results. Inhibition constant of 485.96  $\mu$ M was reported for this docking, as well. As for the RMSD of Cefixime, it was 1.63, which was somewhat lesser than the Cefadroxil and its derivative both. As for the amino acid residues, Asp255A, Asn186A, Thr253A, and Ser116 were involved among all the interactions. Also, there were Arg187A and Lys87 were found to be involved in hydrophobic interaction as seen in (Figure 5).

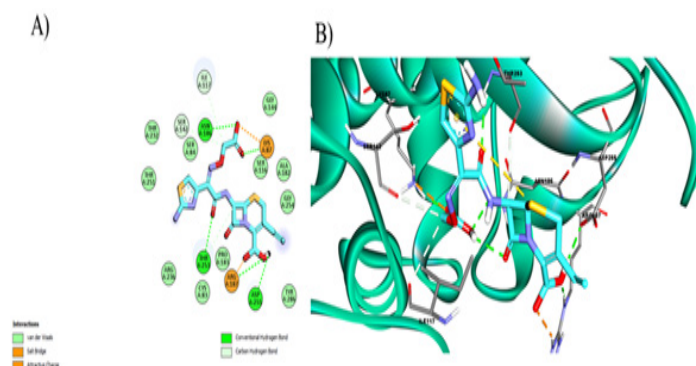


**Figure 5:** Depiction of (a) 2D and (b) 3D interaction of Cefixime with 3N7W protein.

Just as seen in figure (6), the result of the docking of Cefadroxil against the protein 3N7W, the RMSD was found to be at 1.38. The best binding

energy was reported to be at  $-6.09$  Kcal/mol. Other than that, overall in this interaction, amino acids Arg187A, Ser84A, Thr253A, Thr251A, and Ser142A were involved. However, all of these amino acids were involved as the H-bonding forming residues, as well. Lastly, the inhibition constant of this docking was at 34.54.

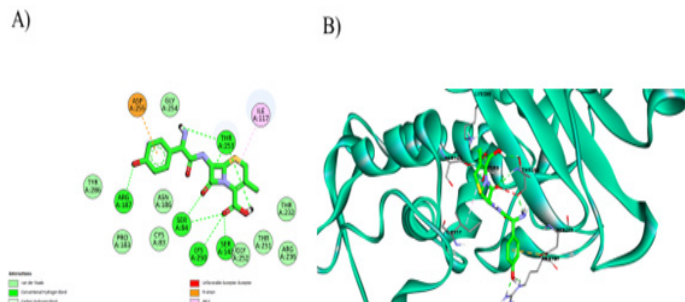


**Figure 6:** Depiction of (a) 2D and (b) 3D interaction of Cefadroxil with 3N7W protein.

In the docking of Cefradine with the 3N7W protein, Asp255A, Ser142A, Ser84A, and Thr253A were found to be involved as H-bond forming residues. Besides that, the RMSD of the docking complex was found to be at 1.08. As for its binding energy, it was found to be at  $-6.00$  Kcal/mol. Other than that, there was the inhibition constant of 39.86. As shown in the (figure 7), amino acids residues Ile117A, Ser142A, Ser84A, and Thr253A were also the ones that were overall involved in the interaction.

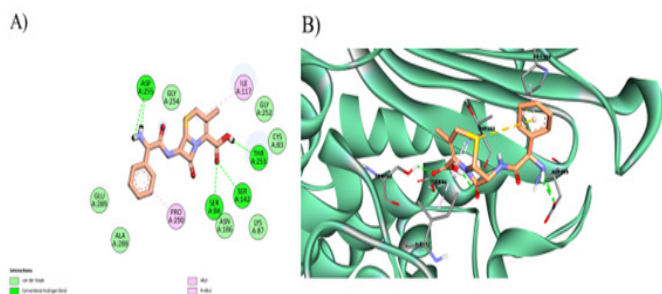


**Figure 7:** Depiction of (a) 2D and (b) 3D interaction of Cefradine with 3N7W protein.

The docking complex of Sulfonamide with the Beta-lactamases protein provided the most excellent results in comparison to all the other drugs. The complex was seen to have the binding energy of  $-8.35$  and an inhibition constant was of about 15.992  $\mu$ M. Its residues Ser84, Thr251, Ser142, Thr253, Ile117, and Lys250 were found to be overall involved in terms of interaction. Figure 8. As for the RMSD, it was reported to be 1.22.

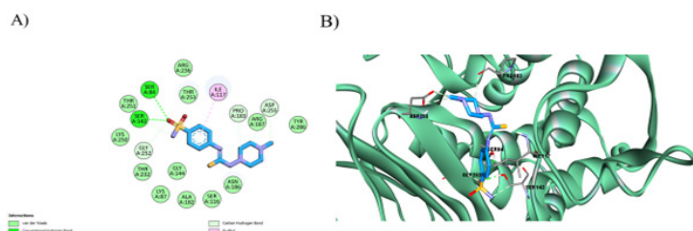


**Figure 8:** Depiction of (a) 2D and (b) 3D interaction of Sulfonamide with 3N7W protein.

## 6.2. Optimization of drugs and Quantum Mechanical Studies

HOMO (highest occupied molecular orbital) – LUMO (lowest unoccupied molecular orbital) energy gaps of chemical species is quietly important descriptors to predict their chemical reactivity and kinetic stability. Low kinetic stability and strong chemical reactivity are typical characteristics of molecules with small frontier orbital gaps. Additionally, such molecules can be described as soft molecules. Moreover, the chemical potential, hardness, and softness are useful tools to find out bioactivity of drug candidates. In our case, the lowest  $\Delta E_{H-L}$  is determined for the compound C2 by the value of 4.4672 eV with the highest chemical softness (18.68 eV) which may be responsible for the higher chemical reactivity.

## 6.3. Derivatives and in their in-silico analysis

### 6.3.1. Cefixime derivative

As for the derivative of Cefixime, its binding energy was calculate to be  $-1.43$ , which is somewhat the lowest as compared to the others. Whereas the RMSD of this docking of Cefixime derivative against the protein was 1.01. Among the H-bond forming residues, only three were involved, which were Lys235 and Ser142. The amount of the inhibition constant was 89170. Overall, the amino acid residues Thr253A, Ser142A, and Ile117A were involved, with Asp255, Pro290, Tyr260, and Ala288 having hydrophobic interaction with the complex as shown in figure (9).

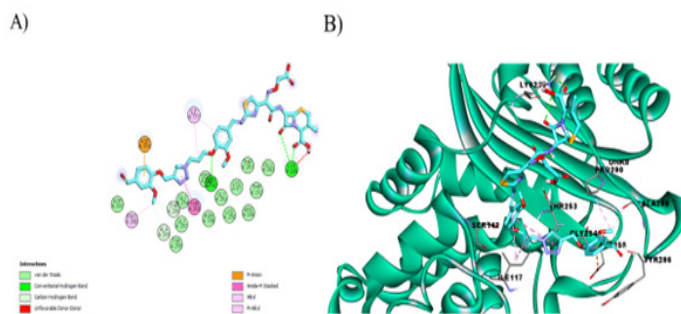


**Figure 9:** Depiction of (a) 2D and (b) 3D interaction of Cefixime derivative with 3N7W protein.

### 6.3.2. Cefadroxil derivative:

Figure (10) shows that among the amino acids that were involved overall in the interaction and as H-bonding forming residues in the docking of Cefadroxil Derivative against 3NA7W protein were Thr232A. There was hydrophobic interaction discovered in the residues Lys87, Ser116, Pro183, and Ala182,. However, the inhibition constant of the docking was 1580 (ki)  $\mu$ M. Whereas, the best binding energy resulted at  $-3.82$  Kcal/mol. The RMSD of the docking was found to be as low as 1.21.

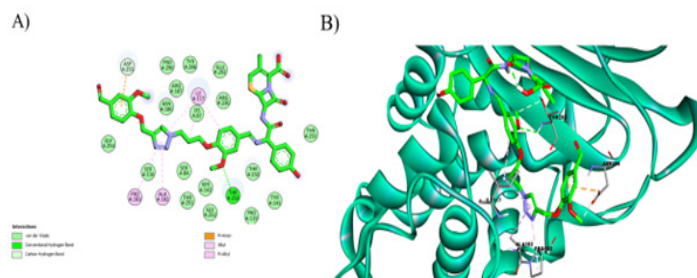


**Figure 10:** Depiction of (a) 2D and (b) 3D interaction of Cefadroxil derivative with 3N7W protein.

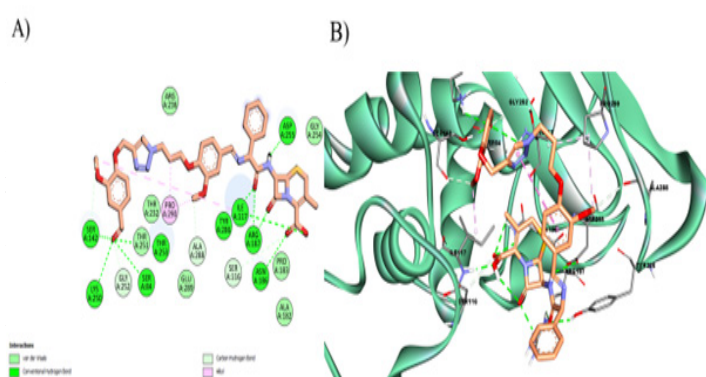


**Figure 11:** Depiction of (a) 2D and (b) 3D interaction of Cefradine derivative with 3N7W protein.

#### 6.3.4. Sulfonamide derivative

In the docking of Sulfonamide derivative with the antibiotic resistance-acquired protein 3N7W, the RMSD was at 1.08. Along with that, the docking also reported a binding energy of -10.22. Then there was the inhibition constant of 11.9922. Among the H-bonding forming residues, Ser84A, Ser116A, Ser142A, IleLys87A, and Glu292A were involved. (Figure 12). Other than that, the residues Thr253A, Ile117A, Pro290A were found to be having hydrophobic interaction with the protein-ligand complex.

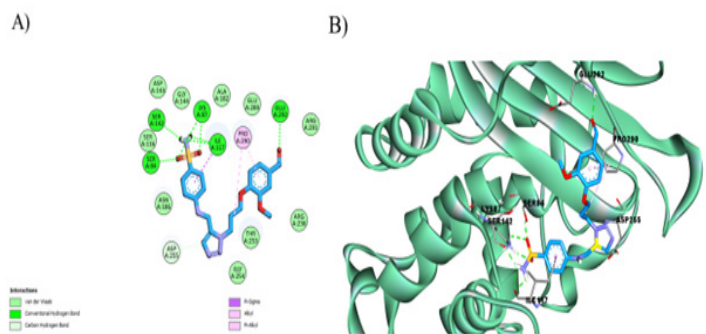


**Figure 12:** Depiction of (a) 2D and (b) 3D interaction of Sulfonamide derivative with 3N7W protein.

#### 6.3.5. Binding Energy and Inhibition Constant of Drugs and Their

#### Derivatives

The  $K_i$ , or inhibitory constant, is a frequently employed indicator of the affinity (strength) with which a medication binds to a specific type (or subtype) of the receptor (also called the inhibition constant). To put it another way, the  $K_i$  stands for the amount of medication (measured in nanomoles, or nM) needed to occupy 50% of those receptors. For instance, the amount of an antipsychotic medicine required to bind to 50% of postsynaptic D2 receptors is known as the  $K_i$ . Therefore, a drug's binding affinity for a certain receptor would be greater the lower the  $K_i$  for that drug at that receptor. This is due to the fact that the lower  $K_i$  shows that even at lower concentrations, the medication may still occupy 50% of those receptors [66].

The improvement of binding affinity, selectivity, and other off-target interactions is a crucial part of hit-to-lead and lead optimization operations in the development of drugs. Relative binding free energy (RBEF) calculations offer an interesting way to predict protein-ligand binding affinities in silico by combining molecular simulations and statistical mechanics to determine the free energy differences across congeneric molecules. RBEF simulations are of particular interest from a computational perspective (for instance, hit-to-lead and lead optimization) due to their accurate modeling of biological systems (such as protein flexibility, explicit solvent, cofactors, ions, concerted motions, and entropy, to name a few), rigorous statistical mechanical framework, and direct application to real-world issues. [67].

From the dockings of the four FDA-approved drugs and their derivatives that were conducted against the 3N7W protein (as shown in fig 13), the **Sulfonamide derivative** was found to have the least binding energy, i.e. -10.22 with its **inhibition constant** being 22.13.

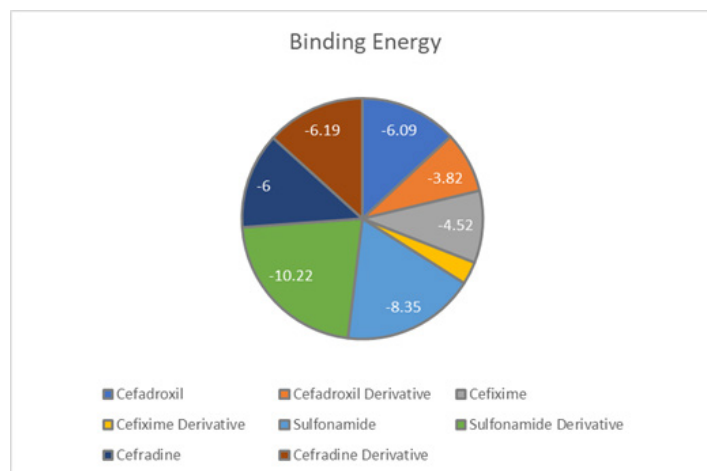


**Figure 13:** Pie chart showing the binding energy of the FDA-approved drugs and their derivatives against 3N7W protein.

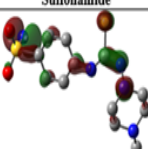
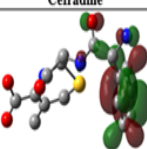
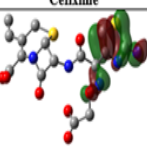
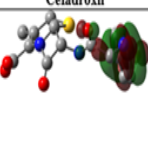
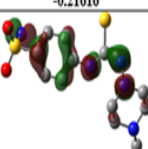
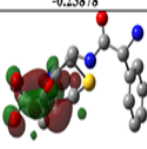
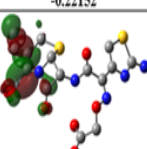
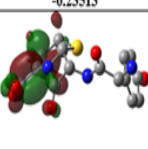
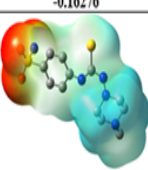
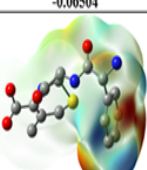
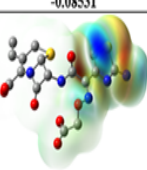
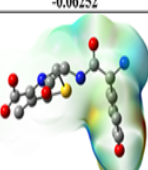
In comparison to that, the **Sulfonamide** was found to have a **binding energy** of -8.35 and an **inhibition constant** of 15.9922 against the 3N7W protein. Whereas the **Cefixime derivative** had the **most binding energy** of -1.43, and its inhibition constant was 89170. The Cefixime itself

was found to have a **binding energy of -4.52** and an **inhibition constant of 485.96**. **Cefadroxil** had an inhibition constant of **34.54** and binding energy of **-6.09**, which is better in comparison to **Cefixime**. The **derivative of Cefadroxil** showed a binding energy of **-3.82**, and its inhibition constant was **1580**. Lastly, the binding energy of **Cefradine** was **-6.00**, along with an inhibition constant of **39.86**.

#### 6.4. Electronic Structure Calculations and HOMO/LUMO Maps of Drugs and Their Derivatives

In order to determine molecular geometries and make predictions about various properties, quantum chemistry techniques are crucial (Anban, James, Kumar, & Pradhan, 2020). The chemically active sites of a molecule are represented by the electron density map with a Molecular Electrostatic Potential (MEP) surface. Understanding chemical reactivity, electrophilic reactions, and substituent effects all heavily depend on electrostatic potential. The MEP can be used to represent the electrostatic characteristics. The design of efficient receptors for anion binding also heavily relies on MEP surface analysis. One of the tools that can be used to develop a linear or bipodal receptor is the MEP surface analysis. For more than 30 years ago, MEP mappings have been logically employed in scientific study. The charge distributions of molecules are shown in three dimensions (3D) on the molecular electrostatic potential surface. These surface investigations let us see a molecule's variously charged areas. Additionally, the MEP surface can be used to map out areas of electron excess and electron deficiency. MEP surface, charge, and dipole may all be created for a particular structure using online tools. (Lakshminarayanan, Jeyasingh, Murugesan, Selvapalam, & Dass, 2021).

As seen in fig.14, the HOMO/LUMO and MEP of the 4 FDA-approved drugs were performed to analyze the drugs and their charge distribution on the quantum level for a better understanding of the properties of these drugs. The results demonstrated that among the four drugs, the charges were evenly distributed throughout the surface of Sulfonamide. Whereas the unequal distribution of charges was found on the surfaces of Cefradine, Cefadroxil, and Cefixime. In accordance with the results that were obtained from the docking study against 3N7W protein, these electronic structures further support Sulfonamide to be a promising drug candidate against MTB.

	Sulfonamide	Cefradine	Cefixime	Cefadroxil
HOMO E(au)	 -0.21616	 -0.23878	 -0.22152	 -0.23513
LUMO E(au)	 -0.16276	 -0.06504	 -0.08531	 -0.06252
MEP				

**Figure 14:** Molecular Electrostatic Potential (MEP) and HOMO/LUMO mapping of the drugs.

#### 6.5. Molecular Dynamics Simulations of Sulfonamide Complex and Its Derivative

It was successful in implementing molecular dynamics simulations to investigate the PBPs enzyme and its complex with the AMPH.

##### 6.5.1. Root Mean Square Deviations (RMSD) of Unbound Protein and the complex

The root mean square deviation (RMSD) of the full trajectory run for the heavy atoms of the enzyme as a function of simulation duration was used to evaluate the conformational stability of all three systems as illustrated in figure (15). The RMSD plot for the ligand-free enzyme is shown in Fig. 6, fluctuating between mean values of  $3.105 \pm 0.01$  Å and  $3.628 \pm 0.11$  Å upon AMPH binding, respectively. This figure illustrates how the enzyme's conformation changes after complex formation. Fig (15). Since RMSDs evaluation showed ligand binding effects on conformational dynamics even at low sampling time.

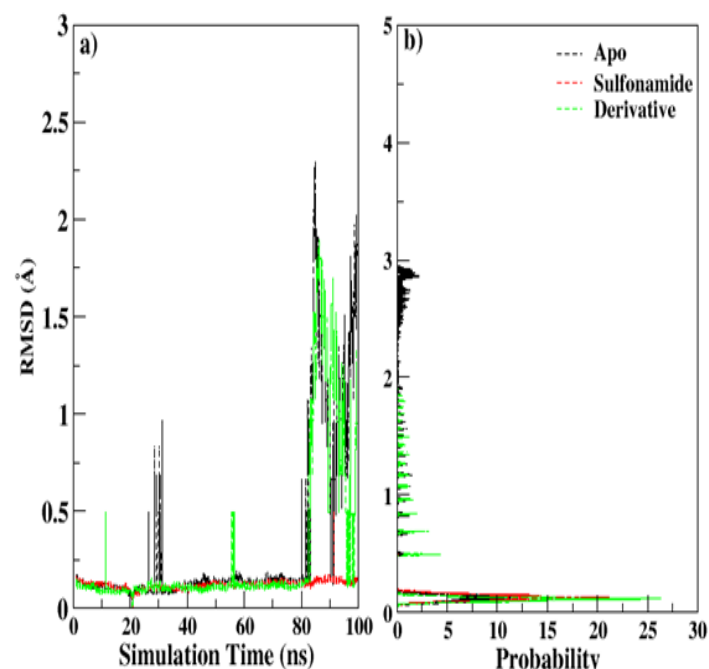


**Figure 15:** Graphs depicting the (a) simulation time and (b) probability plot against RMSD

##### 6.5.2. Root Mean Square Fluctuations (RMSF) of Unbound Protein and the complex

It was urged to further assess the enzyme's dynamical flexibility in its ligand-free and ligand-bound states by the ligand binding effect in the case

of complex formation. As shown in the (RMSF) charts in Fig (16). The sections from amino acid residues in the C terminal trans peptidase domain extend from 80 to 310, and certain portions in the non-penicillin binding domain from 435 to 605. 5.05 with averaged RMSF. This is how the enzyme behaves in the absence of ligand. Since the average RMSF values for the enzyme were calculated to be around 11.81 in the complex case, it was found that the residual dynamics of the enzyme were perturbed by the ligand binding in the case of the complexes, particularly in the regions highlighted region 88 to 122 C-terminal active site domain and 304 to 434 allosteric domain. Particularly for the same amino acid residues, the RMSF pattern for PBPs differed from the ligand-free state; nonetheless, residues involving the binding region exhibited higher variations.

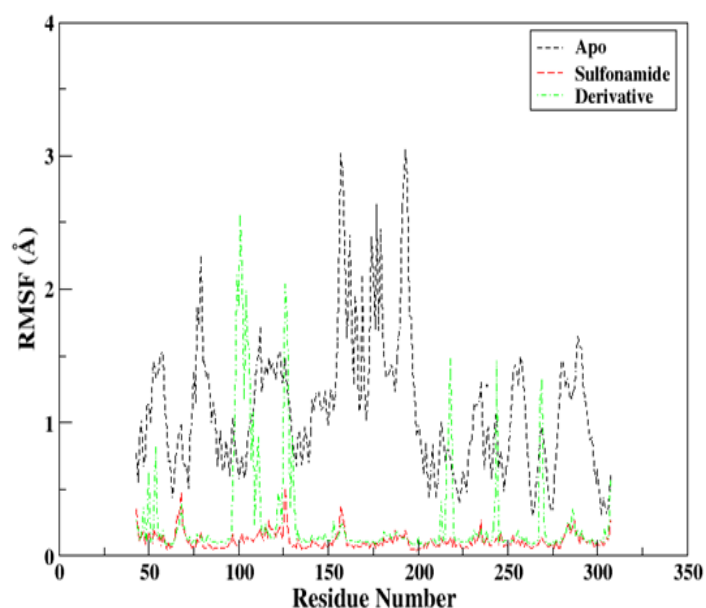
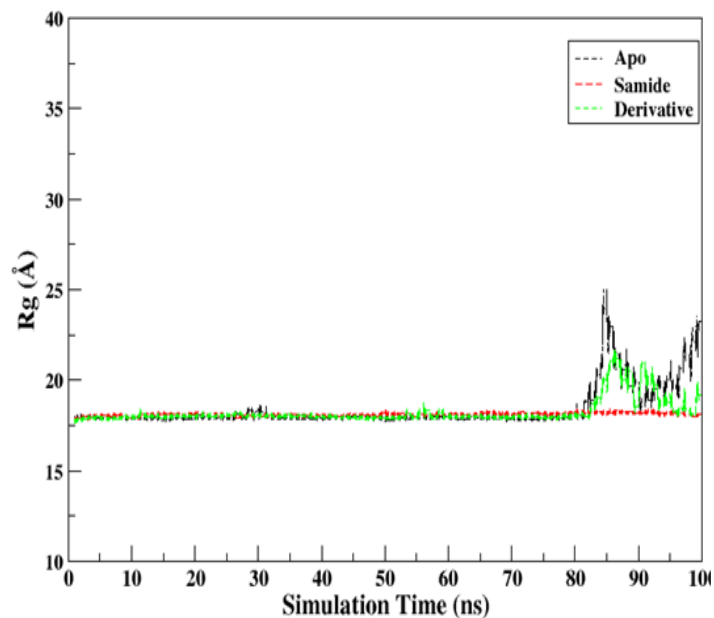


**Figure 16:** Graph depicting the Root Mean Square Fluctuation (RMSF) peaks plotted against residue number

### 6.5.3. Assessment of Compactness of Protein and its Complex

The radius of gyration ( $R_g$ ) is used as a measure of the stability and compactness of protein structures. Consequently, during MD simulations,  $R_g$  values of proteins and complexes were determined. Figure 10(c) makes clear that protein and PBPs-AMPH complexes had various  $R_g$  patterns throughout the simulations. The  $R_g$  of PBPs was clearly seen to be around  $36.48 \pm 0.012$  and  $36.57 \pm 0.015$  as depicted in the figure (17). Radius of gyration results revealed complex formation to slightly decreasing the compactness and increase the gyration of protein and thus confirms the overall disturbance in conformational dynamics of the protein.

**Figure 17:** Molecular Dynamics simulation of Radius of gyration ( $R_g$ ) of the protein without any complex (Apo), complex of protein with Sulfonamide, and complex of protein with Sulfonamide derivative.



### 6.5.4. Hydrogen Analysis

In addition, Hydrogen bond formation potency of simulated complexes were measure in terms number of hydrogen bonds as shown in figure (18) and hydrogen bond cavities depicted in figure (19), where the C 2 compound's enhanced hydrogen bonding was seen with relatively higher bonding cavities, while simulated complexes of ligand 5,6 and 7 were found to have single hydrogen bond with relatively low bonding densities (Fig 18).

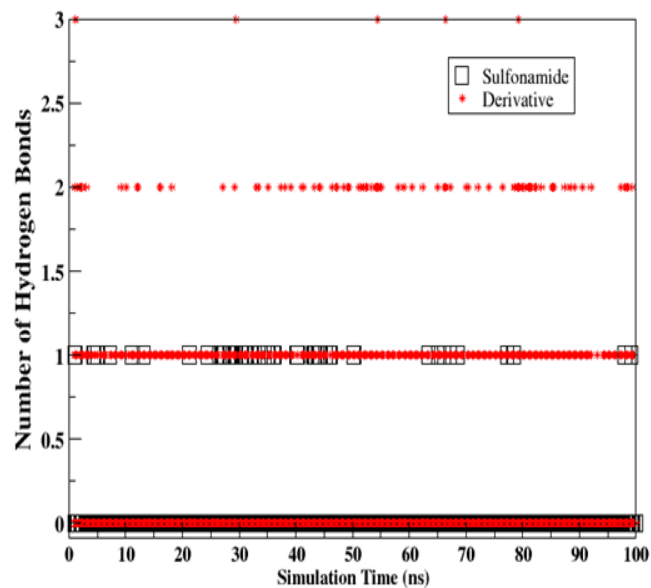


**Figure 18:** Molecular Dynamics hydrogen bond analysis of Sulfonamide and the Sulfonamide derivative.

### 6.5.5. Free Energy of Binding Calculations: MMPBSA

The MM/PBSA methodology is a technique for calculating the binding free energy. With this method, the unbound components as well as snapshots of the complex molecule (derived by MD simulations) are used to average the contributions of gas-phase energy, solvation free energy, and solute entropy.

The binding free energy was determined by the MM/PBSA approach in order to uncover more specific information about the interactions between PBPs and AMPH. In Table 3, the complexes' energy components and a detailed study of their binding free energies are presented. According to the findings, the AMPH had low binding energies. It's interesting that AMPH had the lowest binding energy, at -25 kJ/mol, overall. Four energy components, including van der Waals (DEvdw), electrostatic (DEele), polar solvation energy (DGpol), and nonpolar interactions (DGnonpol), were calculated to better understand which interaction term had the most significant impact on the predicted binding energy. Figure (19) and Table 3's results demonstrate that DEvdw and DEele were significantly engaged in the production of these complexes. It was particularly clear that van der Waals interactions had a significant impact on how well AMPH bound to the chosen molecules. This is because these substances have created significant non-covalent interactions. The polar interaction energies (DEele DGpol) and the non-polar interaction energies (DEvdw DGnonpol) were subsequently determined. Analysis of the data revealed that the selected chemicals and the AMPH binding pocket interact primarily through advantageous non-polar interactions (-25.84 kJ/mol) (Table 3).

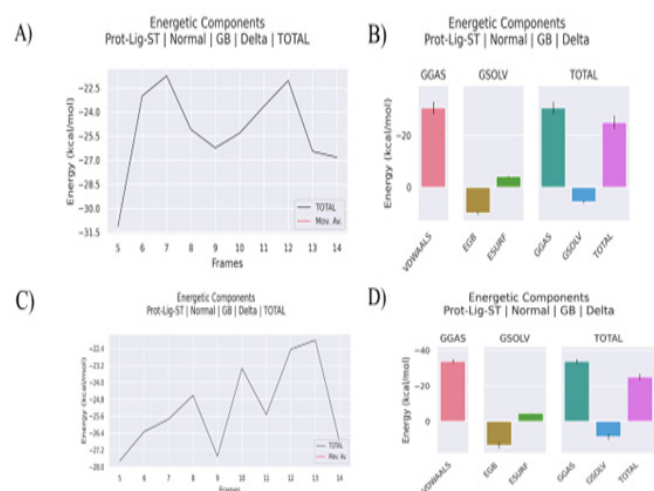


**Figure 19:** (a) Graph depicting the release of binding energy of Sulfonamide with respect to various frames (conformations). (b) Release of different energetic components of Sulfonamide. (c) Graph depicting the release of binding energy of Sulfonamide derivative with respect to various frames (conformations). (d) Release of different energetic components of Sulfonamide derivative.

Energies Kcal/mol	Sulfonamide	Derivative
Vander Waals $\Delta G_{vdw}$	-20.15	-25.20
Vander Waals $\Delta G_{Ele}$	-0.10	-0.80
Surface $\Delta G_{SURF}$	-4.33	-4.67
Solvation $\Delta G_{SOLV}$	-5.56	-8.71
Gaseous $\Delta G_{GAS}$	-5.85	-25.20
Total binding energy $\Delta G_{binding}$	-25.15	-33.91

**Table 3:** Component energies obtained from Sulfonamide and its derivative.

## 7. Conclusion

In recent years, TB has become a fatal disease that is prone to a huge number of drugs and even their derivatives, hence, making itself a health hazard in the years to come. On the other hand, drug repurposing is a process that involves the identification of new therapeutic uses for already existing FDA-approved drugs. The strategy itself is quite effective in discovering or developing new pharmacological therapeutic indications for the drugs. For instant, Aspirin which was used for the treatment of pain, fever, or inflammations has now been repurposed against cardiovascular disorders. The here-presented involved the analysis of the individual interaction of Sulfonamide, Cefradine, Cefadroxil, and Cefixime against the  $\beta$ -lactamases protein using Molecular Docking, MD Simulation, and Quantum Mechanics. In terms of Molecular Docking, Sulfonamide and its derivative were found to have the greatest potency for binding. Whereas the results provided from the Quantum Mechanics analysis revealed higher dipole moment; spread of charge throughout the surface to be the main cause behind the efficacy. As for the MD Simulation, Hydrogen Bond Analysis revealed the Sulfonamide derivative to be forming more hydrogen bonding. Free Energy of Binding revealed the strong binding, confirming the Hydrogen Bonding Analysis revelations. So, the Structure-Activity Relation (SAR) and the above-mentioned data obtained from this study, specifically that of the Sulfonamide drug and its derivative, can be used as a basis on which newer and more effective analogs can be designed to be used against drug-resistance.

## References

1. Connolly LE, Edelstein PH & Ramakrishnan L. Why is long-term therapy required to cure tuberculosis?. *PLoS medicine*. 2007; 4(3): e120.
2. Mishra S, Shukla P, Bhaskar A, Anand K, Baloni P, Jha RK & Singh A. Efficacy of  $\beta$ -lactam/ $\beta$ -lactamase inhibitor combination is linked to WhiB4-mediated changes in redox physiology of Mycobacterium tuberculosis. *Elife*. 2017; 6: e25624.
3. Medeiros AA. Evolution and dissemination of  $\beta$ -lactamases accelerated by generations of  $\beta$ -lactam antibiotics. *Clinical Infectious*

- Diseases, 1997; 24(Supplement\_1), S19-S45.
4. Davies J. Inactivation of antibiotics and the dissemination of resistance genes. *Science*, 1994; 264(5157): 375-382.
  5. Fisher JF, Meroueh SO & Mobashery S. Bacterial resistance to  $\beta$ -lactam antibiotics: compelling opportunism, compelling opportunity. *Chemical reviews*. 2005; 105(2): 395-424.
  6. Flores AR, Parsons LM & Pavelka Jr MS. Genetic analysis of the  $\beta$ -lactamases of *Mycobacterium tuberculosis* and *Mycobacterium smegmatis* and susceptibility to  $\beta$ -lactam antibiotics. *Microbiology*. 2005; 151(2): 521-532.
  7. Wang F, Cassidy C & Sacchettini, J C Crystal structure and activity studies of the *Mycobacterium tuberculosis*  $\beta$ -lactamase reveal its critical role in resistance to  $\beta$ -lactam antibiotics. *Antimicrobial agents and chemotherapy*. 2006; 50(8): 2762-2771.
  8. De Rosa M, Vigliotta G, Palma G, Saturnino C & Soriente A. Novel penicillin-type analogues bearing a variable substituted 2-azetidinone ring at position 6: Synthesis and biological evaluation. *Molecules*. 2015; 20(12): 22044-22057.
  9. González-Bello C, Rodríguez D, Pernas M, Rodríguez Á & Colchón E.  $\beta$ -Lactamase inhibitors to restore the efficacy of antibiotics against superbugs. *Journal of medicinal chemistry*. 2019; 63(5): 1859-1881.
  10. Chambers H. F, Moreau D, Yajko D, Miick C, Wagner C, Hackbarth C & Nikaido H. Can penicillins and other beta-lactam antibiotics be used to treat tuberculosis?. *Antimicrobial agents and chemotherapy*. 1995; 39(12): 2620-2624.
  11. King DT, Sobhanifar S & Strynadka N. C. One ring to rule them all. Current trends in combating bacterial resistance to the  $\beta$ -lactams. *Protein Science*. 2016; 25(4): 787-803.
  12. Kurz S. G & Bonomo RA. Reappraising the use of  $\beta$ -lactams to treat tuberculosis. *Expert review of anti-infective therapy*. 2012; 10(9): 999-1006.
  13. Pushpakom S, Iorio F, Eyers PA, Escott KJ, Hopper S, Wells A, et al. Drug repurposing: progress, challenges and recommendations. *Nat Rev Drug Discovery*. 2019; 18(1): 41-58. doi: 10.1038/nrd.2018.168.
  14. Fatima S, Dwivedi VP. Revisiting Host-Directed Adjunct Therapies in Tuberculosis. *J Bacteriol Mycol* . 2020; 7(4): 1139. doi: 10.1093/cid/civ027.
  15. Nayer H, Steinbach M. Sulfanilamide in clinical tuberculosis. *Am Rev Tuberc*. 1939; 40: 470-2.
  16. Spies HW, Lepper MH, Blatt NH, Dowling HF. Tuberculosis meningitis treatment with streptomycin, para-aminosalicylic acid and promizole, isoniazid and streptomycin, and isoniazid. *Am Rev Tuberc* .1954; 69: 192-204. doi: 10.1164/art.1954.69.2.192
  17. Rashid H, Ahmad N, Abdalla M, Khan K, Martines MAU & Shabana S. Molecular docking and dynamic simulations of Cefixime, Etoposide and Nebrodenside A against the pathogenic proteins of SARS-CoV-2. *Journal of molecular structure*. 2022; 1247: 131296.
  18. Rolinson GN. Forty years of beta-lactam research. *J Antimicrob Chemother*. 1998; 41: 589-603.
  19. Misiek M, Moses AJ, Pursiano TA, Leitner F & Price KE. In vitro activity of cephalosporins against *Mycobacterium tuberculosis* H37Rv: structure-activity relationships. *J Antibiot* (Tokyo). 1973; 26: 737-744.
  20. Moreland RB, Goldstein II, Kim NN, Traish A. Sildenafil Citrate, a Selective Phosphodiesterase Type 5 Inhibitor Trends Endocrinol Metab. *Trends Endocrinol Metabol*. 1999; 10(3): 97-104. doi: 10.1016/s1043-2760(98)00127-1
  21. Singhal S, Mehta J, Desikan R, Ayers D, Roberson P, Eddlemon P, et al. Antitumor activity of thalidomide in refractory multiple myeloma. *N Engl J Med*. 1999; 341(21): 1565-71. doi: 10.1056/NEJM199911183412102. Erratum in: *N Engl J Med* .2000 Feb 3; 342(5): 364. PMID: 10564685.
  22. Field SK. Bedaquiline for the treatment of multidrug-resistant tuberculosis: great promise or disappointment *Ther Adv Chronic Dis*. 2015; 6(4): 170-84. doi: 10.1177/2040622315582325
  23. Conradie F, Diacon AH, Ngubane N, Howell P, Everitt D, Crook AM et al. Treatment of Highly Drug-Resistant Pulmonary Tuberculosis. *N Engl J Med*. 2020; 382(10): 893-902. doi: 10.1056/NEJMoa1901814.
  24. Forgacs P, Wengenack NL, Hall L, Zimmerman SK, Silverman ML, Roberts GD. Tuberculosis and trimethoprim-sulfamethoxazole. *Antimicrob Agents Chemother*. 2009; 53(11): 4789-93. doi: 10.1128/AAC.01658-08
  25. Hasse B, Walker AS, Fehr J, Furrer H, Hoffmann M, Battegay M, et al. Cotrimoxazole prophylaxis is associated with reduced risk of incident tuberculosis in participants in the Swiss HIV Cohort Study. *Antimicrob Agents Chemother*. 2014; 58: 2363-8. doi: 10.1128/AAC
  26. Oladimeji O, Isaakidis P, Obasanya OJ, Eltayeb O, Khogali M, Van den Bergh R, et al. Intensive-phase treatment outcomes among hospitalized multidrug-resistant tuberculosis patients: results from a nationwide cohort in Nigeria. *PLoS One*. 2014; 9: e94393. doi: 10.1371/journal.pone.0094393
  27. Brouqui P, Aubry C, Million M, Drancourt M, Raoult D. Totally resistant tuberculosis: Will antileprosy drugs be helpful? *Int J Antimicrob Agents*. 2013; 42: 584-5. doi: 10.1016/j.ijantimicag.2013
  28. Ameen SM, Drancourt M. In vitro susceptibility of *Mycobacterium tuberculosis* to trimethoprim and sulfonamides in France. *Antimicrob Agents Chemother*. 2013; 57: 6370-1. doi: 10.1128/AAC.01683-13
  29. Abdel-Halim, H., Hajar, M., Hasouneh, L., & Abdelmalek, S. M. Identification of Drug Combination Therapies for SARS-CoV-2: A Molecular Dynamics Simulations Approach. *Drug Design, Development and Therapy*. 2022; 2995-3013. Corinti, Davide, Barbara Chiavarino, Philippe Maitre, Maria Elisa Crestoni, and Simonetta Fornarini.. "Ligation Motifs in Zinc-Bound Sulfonamide Drugs Assayed by IR Ion Spectroscopy" *Molecules*. 2022; 27 no: 10: 3144. Corinti, Davide, Barbara Chiavarino, Philippe Maitre, Maria Elisa Crestoni, and Simonetta Fornarini.. "Ligation Motifs in Zinc-Bound Sulfonamide Drugs Assayed by IR Ion Spectroscopy" *Molecules*. 2022; 27 no: 10: 3144. Hu J, Li X, Liu F, Fu W, Lin L & Li B Comparison of chemical and biological degradation of sulfonamides: Solving the mystery of sulfonamide transformation. *Journal of Hazardous Materials* . 2022; 424: 127661.
  30. Luckner P, & Brandsch M. Interaction of 31  $\beta$ -lactam antibiotics



- with the H<sup>+</sup>/peptide symporter PEPT2: analysis of affinity constants and comparison with PEPT1. *European journal of pharmaceutics and biopharmaceutics*. 2005;59(1): 17-24.
31. Terada T, Saito H, Mukai M, & Inui KI. Recognition of  $\beta$ -lactam antibiotics by rat peptide transporters, PEPT1 and PEPT2, in LLC-PK1 cells. *American Journal of Physiology-Renal Physiology*. 1997;273(5):F706-F711.
  32. Komatsu K, Ito K & Nakajima Y. Kanamitsu Si Imaoka S, Funae Y, Green CE, Tyson CA, Shimada N, Sugiyama Y. Prediction of in vivo drug-drug interactions between tolbutamide and various sulfonamides in humans based on in vitro experiments. *Drug Metab. Dispos.* 2000; 28(4): 475-481.
  33. Mrudula G, Caroline P, Kingsley T, & Jaiswal R. A Review on Drug Interactions in Oral Hypoglycemic Drugs by Mechanism of Cytochrome P450 Enzyme Inhibition. *Journal of Pharmaceutical Research*. 2017; 16(2): 154-159.
  34. Morris G M, & Lim-Wilby M. Molecular docking. *Molecular modeling of proteins*, 2008; 365-382.
  35. Tyagi N, Kumar S, Gangenahalli, G, & Verma Y K. Computational methods (in silico) and stem cells as alternatives to animals in research *Chemoinformatics and Bioinformatics in the Pharmaceutical Sciences*. 2021; (pp. 389-421): Elsevier.
  36. Molecular modelling. (2022, November 21). In Wikipedia.
  37. Stephan S, Horsch MT, Vrabec J, & Hasse H, MolMod—an open access database of force fields for molecular simulations of fluids. *Molecular Simulation*. 2019; 45(10): 806- 814.
  38. Ho TA, & Striolo A. Molecular dynamics simulation of the graphene–water interface: comparing water models. *Molecular Simulation*. 2014;40(14): 1190- 1200.
  39. Lee J, Cheng X, Swails J M, Yeom M S, Eastman P K, Lemkul J A, Qi Y. CHARMM-GUI input generator for NAMD, GROMACS, AMBER, OpenMM, and CHARMM/OpenMM simulations using the CHARMM36 additive force field. *Journal of chemical theory and computation*. 2016;12(1): 405-413.
  40. Arya H & Coumar MS. Lead identification and optimization The Design & Development of Novel Drugs and Vaccines 2021; (pp. 31-63): Elsevier.
  41. Young DC. A practical guide for applying techniques to real-world problems. *Computational Chemistry*, New York. 2001; 9: 390.
  42. Jorgensen WL. The many roles of computation in drug discovery. *Science*, 2004; 303(5665), 1813-1818.
  43. Cavalli A, Carloni P & Recanatini M. Target-related applications of first principles quantum chemical methods in drug design. *Chemical reviews*. 2006;106(9): 3497-3519.
  44. Raha K, Peters MB, Wang B, Yu N, Wollacott AM, Westerhoff LM & Merz KM. The role of quantum mechanics in structure-based drug design. *Drug discovery today*, 2007; 12 (17-18): 725-731.
  45. Peters MB, Raha K & Merz KM. Quantum mechanics in structure-based drug design. *Current opinion in drug discovery & development*. 2006; 9(3): 370- 379.
  46. Thomsen R, & Christensen MH. MolDock: a new technique for high-accuracy molecular docking. *Journal of medicinal chemistry*, 2006;49(11): 3315-3321.
  47. Wizard PP, 2: Epik, Version 2.4, Impact, Version 5.9;(b) GM Satry, M. Adzhigirey, T. Day, R. Annabhimoju and W. Sherman. *J. Comput.-Aided Mol. Des.* 2013; 27: 221- 234.
  48. Sánchez R & Šali A. ModBase: a database of comparative protein structure models. *Bioinformatics*, 1999; 15(12): 1060-1061.
  49. Peitsch MC, Schwede T, & Guex N. Automated protein modelling—the proteome in 3D. *Pharmacogenomics*. 2000; 1(3): 257-266.
  50. Teichmann SA, Murzin AG & Chothia C. Determination of protein function, evolution and interactions by structural genomics. *Current opinion in structural biology*. 2001; 11(3): 354-363.
  51. Tramontano A, Leplae R , & Morea V. Analysis and assessment of comparative modeling predictions in CASP4. *Proteins: Structure, Function, and Bioinformatics*. 2001; 45(S5): 22-38.
  52. Cornell WD, Cieplak P, Bayly CI, Gould IR, Merz KM, Ferguson DM, Kollman PA. A second generation force field for the simulation of proteins, nucleic acids, and organic molecules *J. Am. Chem. Soc.* 1995, 117, 5179- 5197. *Journal of the American Chemical Society*, 1996; 118(9): 2309-2309.
  53. Krieger E & Nabuurs BS & Vriend G. Homology Modeling. 2003,
  54. Bernetti M, Masetti M , Rocchia W, & Cavalli A. Kinetics of drug binding and residence time. *Annual review of physical chemistry*. 2019; 70: 143-171.
  55. Gilson MK, Given JA, Bush BL & McCammon JA. The statistical-thermodynamic basis for computation of binding affinities: a critical review. *Biophysical journal*. 1997; 72(3): 1047-1069.
  56. Copeland RA. The drug–target residence time model: a 10-year retrospective. *Nature Reviews Drug Discovery*. 2016;15(2): 87-95.
  57. Gilson MK, & Zhou H-X. Calculation of protein-ligand binding affinities. *Annu. Rev. Biophys. Biomol. Struct.* 2007 ;36: 21-42.
  58. Kola I, & Landis J. Can the pharmaceutical industry reduce attrition rates? *Nature Reviews Drug Discovery*. 2004; 3(8): 711-716.
  59. Kon K, & Rai M. Antibiotic resistance: mechanisms and new antimicrobial approaches: Academic press. 2016.
  60. Filippova EV, Kieser KJ, Luan CH, Wawrzak Z, Kiryukhina O, Rubin EJ & Anderson WF. (201. 2206-2218): Wiley Online Library.
  61. Kairys, 6). Crystal structures of the transpeptidase domain of the Mycobacterium tuberculosis penicillin-binding protein PonA1 reveal potential mechanisms of antibiotic resistance. 2016; (Vol. 283: pp
  62. Baranauskiene L, Kazlauskienė M, Matulis D & Kazlauskas E. Binding affinity in drug design: experimental and computational techniques. *Expert opinion on drug discovery*, 2019; 14(8), 755-768.
  63. Courmia Z, Allen B, & Sherman W. Relative binding free energy calculations in drug discovery: recent advances and practical considerations. *Journal of Chemical Information and Modeling*. 2017; 57(12), 2911-2937.